Numerical Simulation and Experimental Study on the Dust Separation Performance of the Dust Removal Apparatus in Straw Feed Harvesters

Ziqing Xiao [a,b] Haiqing Tian,[a,b,*] Daqian Wan,[a,b] Chunxiang Zhuo,[a,b] Kai Zhao,[a,b] and Yang Yu [a,b]

* *Corresponding author: hqtian@126.com*

DOI: 10.15376/biores.20.1.1333-1344

GRAPHICAL ABSTRACT

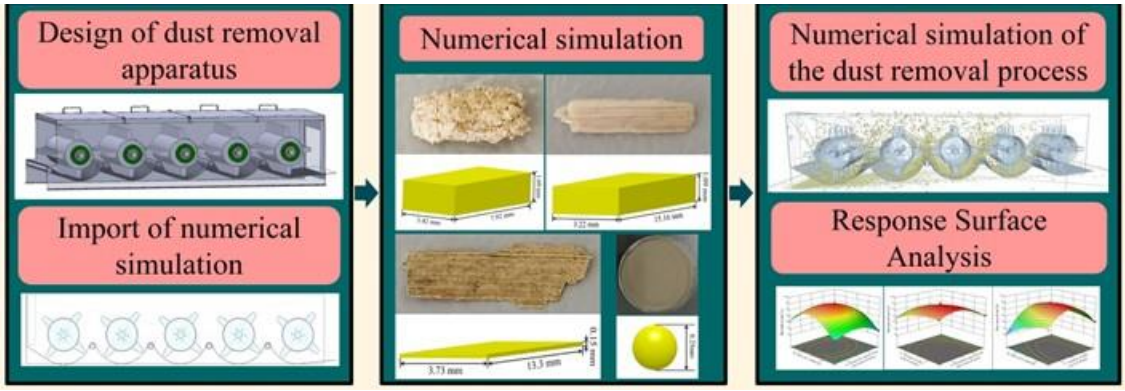

Numerical Simulation and Experimental Study on the Dust Separation Performance of the Dust Removal Apparatus in Straw Feed Harvesters

Ziqing Xiao [a,b] Haiqing Tian,[a,b,*] Daqian Wan,[a,b] Chunxiang Zhuo,[a,b] Kai Zhao,[a,b] and Yang Yu [a,b]

To address the issue of excessive soil content in straw feed after harvesting by a straw feed harvester, this study designed a dust removal apparatus. Its optimal operating parameters were determined through a combination of numerical simulations and field experiments. Using dust removal efficiency as the evaluation criterion, the Box-Behnken experiment and variance analysis revealed that the factors influencing the dust removal efficiency of the apparatus, in order of significance, were the number of dust removal drums, the aperture of the dust sieve, and the rotational speed of the dust removal drums. The optimal parameter combination consisted of 5 dust removal drums, a dust sieve aperture of 5 mm, and a drum rotational speed of 370 r/min. The dust removal efficiency obtained from numerical simulation using these optimal parameters was 94.1%, while the field verification test yielded an efficiency of 93.5%, with a relative error of 0.64% between the two results, confirming the accuracy of the numerical simulation parameters. The optimized dust removal apparatus significantly improves the quality of straw fodder by reducing dust content, which not only enhances the efficiency of straw recycling but also supports sustainable agricultural practices, promoting both mechanization and green development in the industry.

DOI: 10.15376/biores.20.1.1333-1344

Keywords: Dust removal apparatus; Straw feed; Numerical simulation; Field experiment; Dust separation

Contact information: a: College of Mechanical and Electrical Engineering, Inner Mongolia Agricultural University, Hohhot, 010018, China; b: Inner Mongolia Engineering Research Centre of Intelligent Equipment for the Entire Process of Forage and Feed Production, Hohhot 010018, China;
** Corresponding author: hqtian@126.com*

INTRODUCTION

Maize is one of the most widely produced cereal crops globally (Ren *et al*. 2022; Yu *et al*. 2024), and after harvesting, maize stalks are typically utilized in two primary ways: harvested during the milk to dough stage for use as silage (Tao *et al*. 2024; Xue *et al*. 2024; Zhao *et al*. 2024), or harvested post-maturity for use as dry forage (Li *et al*. 2022; Mu *et al*. 2024; Wang *et al*. 2024). The maize stalks, harvested by the forage harvester, can be directly converted into dry forage suitable for feeding livestock. However, during the harvesting process, a significant amount of dust is mixed into the feed, reducing its quality. Therefore, designing and developing a dust removal apparatus to separate dust mixed into the forage is a critical step in improving feed quality. However, traditional research methods are insufficient to accurately analyze the movement and separation behavior of dust particles within the apparatus. In recent years, the Discrete Element Method (DEM),

as a numerical simulation tool, has become an essential approach for addressing complex problems that traditional methods struggle to resolve, due to its ability to thoroughly investigate contact mechanics and tribology between particles (Fang *et al*. 2022; Du *et al*. 2023; Walunj *et al*. 2023; Li *et al*. 2024). This method is widely used to obtain complex behavior information that is difficult to measure, such as particle motion, forces, and energy consumption during material breakage (Ma *et al*. 2015, 2019; Zhou *et al*. 2023).

The harvested straw fodder appears as a mixture consisting of segmented straw rind, segmented straw pith, powdered straw rind, powdered straw pith, and dust particles. Removing the dust from this mixture using a dust removal apparatus can significantly improve the feed's cleanliness, thereby enhancing its utilization efficiency. Although significant research has been conducted on agricultural product separation (Chen *et al*. 2010), the focus has primarily been on peeling, screening, and analyzing the motion of agricultural particles (Fan *et al*. 2022). For example, Chen *et al*. (2022) combined computational fluid dynamics (CFD) and the discrete element method (DEM) to simulate the separation process of rice grains and husks, revealing the mechanisms behind grain loss and husk retention. Wang *et al*. (2023) utilized the CFD-DEM method to simulate and validate the screening process of maize mixtures, analyzing the behavior of maize particles passing through bionic sieve apertures under various orientations. However, studies on the dust removal mechanism for forage mixtures of maize stalks remain limited, with little focus on the dynamic interactions between the forage and dust during the separation process.

This study describes a dust removal apparatus for the forage harvester and investigates the motion and separation of forage mixtures inside the apparatus using a combination of numerical simulation and experimental validation. The dust removal efficiency was used as the evaluation metric, with the rotational speed of the dust removal drum, the sieve aperture size, and the number of dust removal drums as experimental factors. A three-factor, three-level orthogonal numerical simulation experiment was conducted to determine the optimal operating parameters for the dust removal apparatus. The effectiveness and stability of the apparatus were validated through field experiments, providing a critical basis for further improving dust removal efficiency and optimizing the apparatus design. The primary objective of this study was to optimize the operational parameters of the dust removal apparatus to significantly reduce the dust content in straw fodder, improve its quality, and provide technical support for the utilization of straw resources in agricultural mechanization. Additionally, this study aimed to provide a theoretical basis for the further improvement and application of the dust removal apparatus.

EXPERIMENTAL

Test Material

The straw fodder was sourced from the experimental field in Dageben Village, Tumed Left Banner, Hohhot City, Inner Mongolia Autonomous Region (121°58'E, 36°15'N) after the harvesting operation. According to the GB/T 5917.1 (2008) standard, the straw fodder was sieved using a standard sieve. The sieved material included segmented straw rind and pith, powdered straw rind and pith, as well as dust particles. The powdered straw rind and pith had a cylindrical shape. The dimensions of the sieved materials were measured using an ABS digital caliper (Yantai Lulin Tools Co., Ltd., Shandong, China), and the average values were calculated. The particle size distribution of the dust was

determined using a Bettersize 3000Plus laser particle size analyzer (Dandong Bettersize Instruments Ltd., Liaoning, China), and the average value was obtained. The components were dried using a DHG-9245A forced air drying oven (Shanghai Yiheng Scientific Instrument Co., Ltd., Shanghai, China). The moisture content of each component was then measured using the gravimetric method, and the average value was calculated. The composition, physical properties, moisture content, and proportions are listed in Table 1.

Table 1. Composition and Proportions of the Forage Mixture

Composition	Length (mm)	Width (mm)	Thickness (mm)	Diameter (mm)	Moisture Content (%)	Proportion (%)
Segmented straw rind	15.16	3.22	1.09		10.2	35.5
Segmented straw pith	7.92	3.42	1.69		10.2	34.7
Powdered straw rind	5.82			0.93	10.2	12.3
Powdered straw pith	3.21			1.45	10.2	14.5
Dust				0.25	7.3	3

Test Apparatus

The designed dust removal apparatus for the forage harvester is shown in Fig. 1. The main working components include the trapezoidal blade, dust removal drum, dust removal apparatus casing, drum shaft, rear sieve, middle sieve, and front sieve. The forage enters the dust removal apparatus through the front sieve, where the rotating dust removal drum drives the trapezoidal blade to continuously toss the feed into the subsequent working unit. As the feed is tossed and rubbed against the underlying sieve, separation from the dust occurs, with the dust being discharged through the bottom sieve.

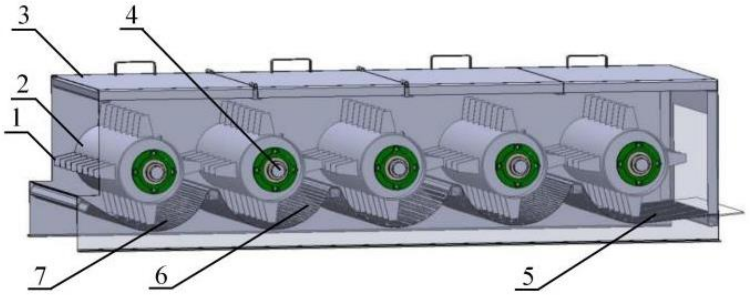

Fig. 1. Schematic diagram of dust removal apparatus: (1-trapezoidal blade; 2-dust removal drum; 3-dust removal apparatus housing; 4-dust removal drum shaft; 5-rear screen; 6-middle screen; 7-front screen)

The designed dust removal apparatus was imported into EDEM (Altair Engineering Inc., MI, USA, 2023), with the model dimensions being 2435 mm in length, 925 mm in width, and 585 mm in height. The rotation direction and speed were set at the center of the axis of the dust removal drum. The particle factory was positioned at the inlet of the dust removal apparatus to simulate the state when the straw fodder harvester transports fodder to the dust removal apparatus. A plane was established below the model, with dimensions of 3,000 mm in length and 1,000 mm in width, to record the mass of dust particles after the dust removal simulation, as shown in Fig. 2.

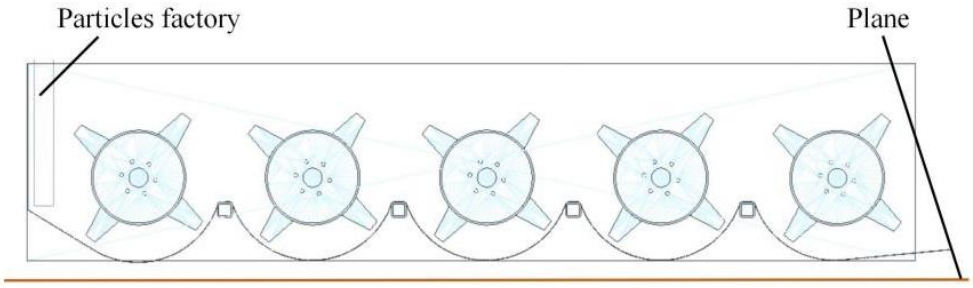

Fig. 2. Numerical simulation model of dust removal apparatus

Test Method

Based on the screening results and proportions of the straw mixture shown in Table 1, a dust removal simulation test was performed using the EDEM software (Altair Engineering Inc., MI, USA, 2023). A total of 6,000 g of particles were generated, including segmented straw rind particles, segmented straw pith particles, powdered straw rind particles, powdered straw pith particles, and dust particles. The respective proportions of these particles were 35.5%, 34.7%, 12.3%, 14.5%, and 3%. The segmented straw rind particles and segmented straw pith particles were modeled as polyhedral particles (Fig. 3 a~b), while the powdered straw rind and powdered straw pith particles were modeled as cylindrical (Fig. 3 c~d). Dust particles were modeled as spherical particles (Fig. 3 e). Due to the adhesion forces between the particles in the fodder mixture, the Hertz-Mindlin with JKR contact model was selected for the numerical simulation. The dust removal apparatus model was made of steel. The basic physical parameters of the models are presented in Table 2, and the contact parameters (Feng *et al*. 2021; Xiao *et al*. 2022) are shown in Table 3.

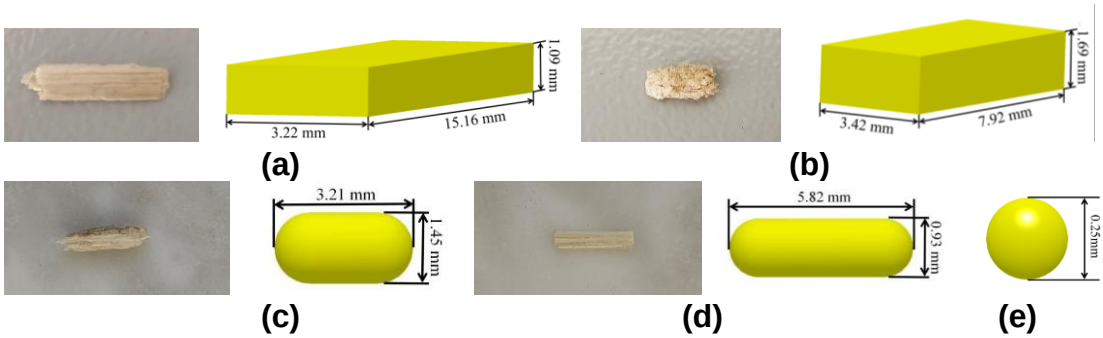

Fig. 3. Numerical simulation models of the various particles:(a-the actual segmented straw rind and its particle model; b-the segmented straw pith and its particle model; c- the powdered straw rind particles and its particle model; d- the powdered straw pith particles and its particle model; e- the dust particle model)

Table 2. Numerical Simulation Model Parameters

Particle Type	Poisson's ratio	Density (kg/m^3)	Shear modulus (MPa)
Straw bract	0.219	989	2.3
Straw pith	0.3	40	64
Straw rind	0.4	508	2270
Steel	0.3	7865	79000
Dust	0.4	2600	11.5

Table 3. Contact Parameters Between Particles

Particle model	Static friction	Dynamic friction	Restitution coefficient	JKR surface energy coefficient
pith-pith	0.427	0.144	0.348	0~0.2
pith-rind	0.495	0.166	0.263	0~0.2
pith-steel	0.375	0.15	0.325	/
rind-rind	0.142	0.078	0.485	0~0.2
rind-steel	0.226	0.119	0.663	/
dust-pith	0.75	0.45	0.135	0~0.2
dust-rind	0.55	0.35	0.213	0~0.2
dust-dust	0.74	0.182	0.52	9.052
dust-steel	0.85	0.125	0.35	/

The dust removal efficiency was used as the evaluation criterion, with the rotational speed of the dust removal drum, sieve aperture, and the number of dust removal drums as the factors for the numerical simulation. A three-factor, three-level orthogonal simulation experiment was conducted, with each factor categorized into low (-1), medium (0), and high (1) levels using a Box-Behnken experimental design. The simulation factors and evaluation criteria for dust removal are presented in Table 4. Three center points were used to assess experimental error, and a total of 15 numerical simulations were performed.

Table 4. Numerical Simulation of Dust Removal Experiment Factors and Parameters

Factor	Low Level (-1)	Medium Level (0)	High Level (1)
Rotational speed of the dust removal drum X_1	270	370	470
Dust sieve aperture X_2	3	5	7
Number of dust removal drums X_3	4	5	6

RESULTS AND DISCUSSION

Analysis of the Numerical Simulation Process

By using EDEM software, the motion trajectories and interaction processes between straw fodder particles and dust particles were visualized, simulating the dynamic movement of straw fodder within the dust removal apparatus. This simulation provides analysis of particle separation and dust removal efficiency, as shown in Fig. 4.

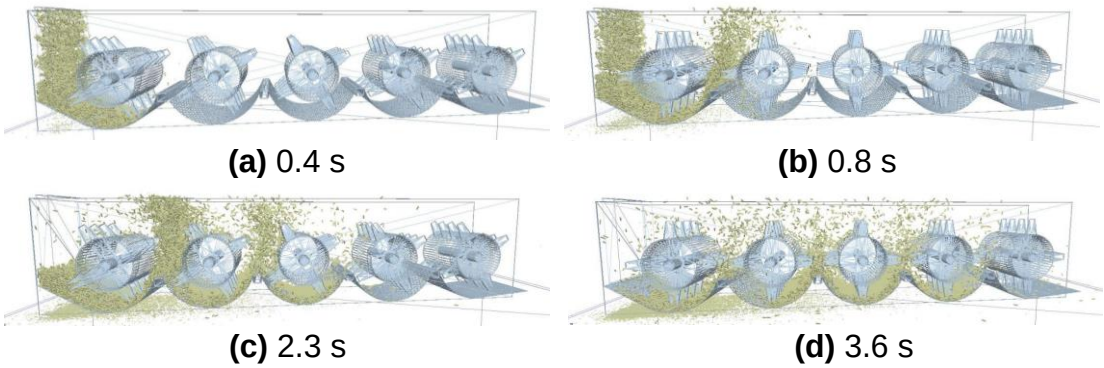

(a) 0.4 s **(b)** 0.8 s **(c)** 2.3 s **(d)** 3.6 s

Fig. 4. Numerical simulation results at different time intervals

The motion of straw fodder particles in the numerical simulation followed a parabolic trajectory, with each stage of the dust removal apparatus propelling the fodder no further than the radius of the dust removal drum. The straw fodder was propelled step-by-step through each stage of the dust removal apparatus, with no instances of cross-stage transportation, resulting in effective dust removal. The motion state of the straw fodder met the design requirements, and the numerical simulation experiment demonstrated that the designed dust removal apparatus can meet the basic dust removal requirements for straw fodder.

Box-Behnken Experimental Design and Response Surface Analysis

The Box-Behnken experimental design and results of the numerical simulation dust removal tests for the dust removal apparatus are presented in Table 5.

Table 5. Box-Behnken Experimental Design and Results

Serial Number	X_1	X_2	X_3	Dust removal α (%)
1	0 (370)	0 (5)	0 (5)	94.31
2	0 (370)	-1 (3)	-1 (4)	84.5
3	0 (370)	-1 (3)	1 (6)	70.17
4	0 (370)	1 (7)	-1 (4)	81.48
5	1 (470)	-1 (3)	0 (5)	73.75
6	-1 (270)	-1 (3)	0 (5)	77.84
7	1 (470)	0 (5)	-1 (4)	86.74
8	-1 (270)	0 (5)	-1 (4)	92.09
9	0 (370)	1 (7)	1 (6)	85.1
10	1 (470)	0 (5)	1 (6)	81.67
11	-1 (270)	0 (5)	1 (6)	83.42
12	0 (370)	0 (5)	0 (5)	94.18
13	1 (470)	1 (7)	0 (5)	75.64
14	0 (370)	0 (5)	0 (5)	95.65
15	-1 (270)	1 (7)	0 (5)	80.85

A multivariate regression analysis was performed on the results using Design-Expert software, yielding a quadratic polynomial equation that relates the experimental factors to the dust removal efficiency in the numerical simulation tests:

$$\alpha = 94.7-2.05X_1+2.10X_2-3.06X_3-0.28X_1X_2+0.90X_1X_3+4.49X_2X_3$$
$$-6.01X_1^2-11.68X_2^2-2.72X_3^2 \quad (1)$$

Variance analysis was conducted for the Box-Behnken experiment, and the statistical results are presented in Table 6. As shown in Table 6, the rotational speed of the dust removal drum (X_1), dust sieve aperture (X_2), number of dust removal drums (X_3), interaction between the dust sieve aperture and the number of drums (X_2X_3), the quadratic terms of the drum's rotational speed (X_1^2), and the sieve aperture (X_2^2) all showed highly significant effects on the dust removal efficiency. Additionally, the quadratic term of the number of drums (X_3^2) had a significant effect. The model's P-value was less than 0.01, indicating a highly significant relationship between the dust removal efficiency and the regression equation. The lack-of-fit P-value of 0.2076, being greater than 0.05, suggests that the model fit the data well. A coefficient of variation of 1.62% indicates a high level of experimental reliability. The coefficient of determination R^2 was 0.9891, and the adjusted R^2 was 0.9695, both of which are close to 1, indicating that the model accurately

reflected the actual situation. Based on the P-values, the decreasing order of influence of the experimental factors on dust removal efficiency was as follows: number of dust removal drums, dust sieve aperture, and rotational speed of the dust removal drum.

Table 6. Variance Analysis of the Regression Model for the Box-Behnken Experimental Design

Source of variation	Sum of squares	Degrees of freedom	Mean square	P-value
Model	836.60	9	92.26	0.000 2**
X_1	33.62	1	33.62	0.007 9**
X_2	35.32	1	35.32	0.007 2**
X_3	74.73	1	74.73	0.001 4**
X_1X_2	0.31	1	0.31	0.697 1
X_1X_3	3.24	1	3.24	0.242 3
X_2X_3	80.55	1	80.55	0.001 2**
X_1^2	133.50	1	133.50	0.000 4**
X_2^2	503.75	1	503.75	<0.000 1**
X_3^2	27.33	1	27.33	0.012 0*
Residual	9.22	5	1.84	
Lack of fit	7.90	3	2.63	0.2076
Pure error	1.32	2	0.66	
Sum	845.82	14		

Note: * indicates significant influence ($0.01 \leqslant P < 0.05$), ** indicates highly significant influence ($P < 0.01$).

Design-Expert software was used to analyze the interactions between different factors, and the corresponding response surface and contour plots were generated. The response surface for the interaction between the rotational speed of the dust removal drum and the dust sieve aperture (X_1X_2) on dust removal efficiency are shown in Fig. 5(a). From the figure, it is evident that the surface slope changed significantly, indicating that parameters X_1 and X_2 had a considerable effect on the dust removal efficiency. The response surface depicting the interaction effect of the rotational speed of the dust removal drum (X_1) and the number of dust removal drums (X_3) on the dust removal efficiency is shown in Figure 5(b). The response surface and contour plot illustrating the interaction between the dust sieve aperture (X_2) and the number of dust removal drums (X_3) on dust removal efficiency are shown in Figure 5(c). The figure shows significant variation in the surface slope, indicating that parameters X_2 and X_3 had a substantial effect on dust removal efficiency.

The response surface of the interaction among factors reveals that the dust removal efficiency initially increased and then decreased as the rotational speed of the dust removal drum, dust sieve aperture, and the number of dust removal drums progressively increased. By comparing the slopes of the response surfaces, it can be concluded that the factors influencing dust removal efficiency, in decreasing order of significance, were the number of dust removal drums, the dust sieve aperture, and the rotational speed of the dust removal drum. As shown in Fig. 5, the red area in the center of the response surface indicates that the highest dust removal efficiency was achieved at the 0 level of each experimental factor. The optimal parameter values were as follows: dust removal drum rotational speed of 370 r/min, sieve aperture of 5 mm, and five dust removal drums. Using these optimal parameters, three repeated numerical simulation experiments were conducted, yielding dust removal efficiencies of 93.97%, 94.15%, and 94.18%, with an average dust removal efficiency of 94.1%.

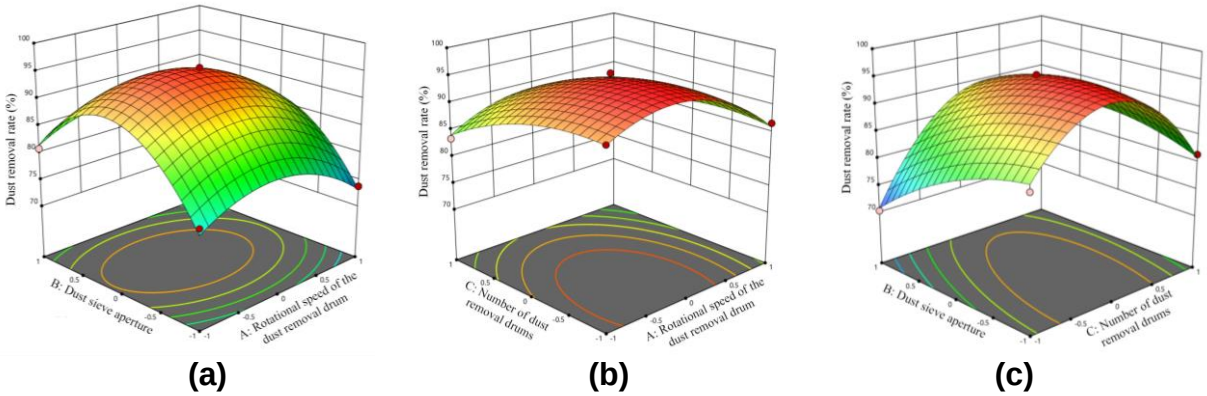

Fig. 5. Response surfaces illustrating the interaction effects among various factors: (a-the interaction between factors X_1 and X_2; b-the interaction between factors X_1 and X_3; c-the interaction between factors X_2 and X_3)

Field Performance Tests

The optimal parameters for the dust removal apparatus, obtained from the numerical simulation test, were a dust removal drum rotational speed of 370 r/min, a dust sieve aperture of 5 mm, and five dust removal drums. Based on these parameters, a drum-type dust removal apparatus was fabricated, as shown in Fig. 6, and installed on the straw fodder harvester, as shown in Fig. 7. The field performance validation test was conducted in Liuer Ying Village, Hohhot, Inner Mongolia Autonomous Region. The test materials consisted of post-harvest baled straw fodder with an average moisture content of 13.8%.

Fig. 6. The physical structure of the dust removal apparatus

During the dust removal experiment, the straw fodder was weighed using a scale to determine its mass, and the initial mass, m_1, was recorded. The straw fodder with the known initial mass was then spread evenly on the ground, and the straw fodder harvester carried out the picking and dust removal operation. The experimental process is illustrated in Fig. 8. The straw fodder that had passed through the dust removal apparatus was collected and weighed, and its post-removal mass, m_2, was recorded. During the dust removal operation, a small portion of the smaller-diameter straw fodder fell to the ground along with the dust. The fallen straw was collected, washed, dried, and its mass, m_3, was recorded. A small amount of dust remained in the post-removal fodder, which was subsequently washed and dried, and its mass, m_4, was recorded.

The dust removal efficiency (α) of the dust removal apparatus can be calculated using Eq. 2,

$$\alpha = (1 - \frac{m_2 - m_4}{m_1 - m_3 - m_4}) \times 100\% \quad (2)$$

where m_1 is the initial mass of the straw fodder (g), m_2 is the mass of the straw fodder after dust removal (g), m_3 is the mass of the straw fodder that fell to the ground during the dust removal process (g), and m_4 is the mass of the dust-free straw fodder (g).

Fig. 7. Field test procedure

During the experiment, the dust removal efficiency of the apparatus was tested at three different rotational speeds. For each speed, straw fodder of three different masses was collected for the field test. The dust removal efficiencies obtained from the tests are shown in Table 7. As shown in Table 7, the dust removal efficiency was highest at a rotational speed of 370 r/min, reaching 93.50%. The dust removal efficiency from the numerical simulation test was 94.10%, and the relative error between the two was 0.64%, confirming the accuracy of the numerical simulation test parameters.

Table 7. Impurity Content Rate in the Field Test

Rotational Speed/r·min^{-1}	Initial Mass of Straw Fodder (g)	Mass of Straw Fodder After Dust Removal (g)	Mass of Straw Fodder Fallen to Ground During Dust Removal (g)	Dust-Free Mass of Straw Fodder (g)	Dust Removal Efficiency (%)	Average Dust Removal Efficiency (%)
270	40 000	34 200	3 672	33 920	88.37	87.60
	50 000	43 400	4 232	43 046	87	
	60 000	51 950	5 396	51 568	87.42	
370	40 000	33 250	2 954	32 994	93.68	93.50
	50 000	41 500	4 136	41 178	93.11	
	60 000	50 050	4 144	49 660	93.71	
470	40 000	35 350	2 014	35 058	85.50	86.29
	50 000	43 500	3 962	43 114	86.80	
	60 000	52 450	4 596	51 992	86.58	

CONCLUSIONS

1. Using the Box-Behnken design in Design-Expert software, the significance ranking of the factors affecting the dust removal efficiency of the dust removal apparatus was determined. The most significant factors, in order, were the number of dust removal drums, the dust sieve aperture, and the rotational speed of the dust removal drum.
2. Using dust removal efficiency as the evaluation metric, the Box-Behnken design and analysis of variance were employed to determine the optimal parameter values. The optimal solution was found to be: 5 dust removal drums, a dust sieve aperture of 5 mm, and a dust removal drum rotational speed of 370 r/min.
3. The dust removal efficiency obtained from the numerical simulation test, conducted using the optimal parameters, was 94.1%. The field validation test yielded a dust removal efficiency of 93.5%. The relative error between the two results was 0.64%, confirming the accuracy of the parameters used in the numerical simulation.

ACKNOWLEDGMENTS

The authors are grateful for the funding support of the National Natural Science Foundation of China [Grant No.52365035], the National Natural Science Foundation of China [Grant No.32071893], the Inner Mongolia Autonomous Region Science and Technology Projects [Grant No.2022YFDZ0024], and the First-class Discipline Research Special Projects of the Inner Mongolia Autonomous Region [Grant No.YLXKZX-NND-046].

REFERENCES CITED

Chen, P., Han, Y., Jia, F., Zhao, D., Meng, X., Li, A., Chu, Y., and Zhao, H. (2022). "Investigation of the mechanism of aerodynamic separation of rice husks from brown rice following paddy hulling by coupled CFD-DEM," *Biosystems Engineering* 218, 200-215. DOI: 10.1016/j.biosystemseng.2022.03.015

Chen, Y.-S., Hsiau, S.-S., Lee, H.-Y., Chyou, Y.-P., and Hsu, C.-J. (2010). "Size separation of particulates in a trommel screen system," *Chemical Engineering and Processing: Process Intensification* 49(11), 1214-1221. DOI: 10.1016/j.cep.2010.09.003

Du, X., Liu, C., Liu, C., Sun, Q., and Chen, S. (2023). "A novel method for measurement of the angle of repose of granular seeds in discrete element methods," *Journal of Agricultural Engineering* 54(2). DOI: 10.4081/jae.2023.1504

Fan, M., Su, D., and Yang, L. (2022). "Development of a benchmark for drag correlations of nonspherical particles based on settling experiments of super-ellipsoidal particles," *Powder Technology* 409, article 117811. DOI: 10.1016/j.powtec.2022.117811

Fang, M., Yu, Z., Zhang, W., Cao, J., and Liu, W. (2022). "Friction coefficient calibration of corn stalk particle mixtures using Plackett-Burman design and response surface methodology," *Powder Technology* 396, 731-742. DOI: 10.1016/j.powtec.2021.10.040

Feng, X., Liu, T., Wang, L., Yu, Y., Zhang, S., and Song, L. (2021). "Investigation on JKR surface energy of high-humidity maize grains," *Powder Technology* 382, 406-419. DOI: 10.1016/j.powtec.2020.12.051

Li, D., Tian, H., Sheng, Y., Ren, X., and Zhou, J. (2022). "Experimental and influencing factors of corn stalk pulling force," *Engenharia Agrícola* 42(5), article e20210219. DOI: 10.1590/1809-4430-eng.agric.v42n5e20210219/2022

Li, S., Diao, P., Miao, H., Zhao, Y., Li, X., and Zhao, H. (2024). "Modeling the fracture process of wheat straw using a discrete element approach," *Powder Technology* 439, article 119726. DOI: 10.1016/j.powtec.2024.119726

Ma, X., Guo, B., and Li, L. (2019). "Simulation and experiment study on segregation mechanism of rice from straws under horizontal vibration," *Biosystems Engineering* 186, 1-13. DOI: 10.1016/j.biosystemseng.2019.06.015

Ma, Z., Li, Y., and Xu, L. (2015). "Discrete-element method simulation of agricultural particles' motion in variable-amplitude screen box," *Computers and Electronics in Agriculture* 118, 92-99. DOI: 10.1016/j.compag.2015.08.030

Mu, Q., Tian, H., Xiao, Z., Zhuo, C., Xue, X., and Tang, L. (2024). "Vibration testing and analysis of the pickup header of straw forage harvester under multi-source excitation," *INMATEH Agricultural Engineering* 324-337. DOI: 10.35633/inmateh-73-27

Ren, X., Tian, H., Zhao, K., Li, D., Xiao, Z., Yu, Y., and Liu, F. (2022). "Research on pH value detection method during maize silage secondary fermentation based on computer vision," *Agriculture* 12(10), article 1623. DOI: 10.3390/agriculture12101623

Tao, Y., Tian, H., Zhao, K., Yu, Y., Guo, L., Liu, G., and Bai, X. (2024). "High-precision discrimination of maize silage based on olfactory visualization technology integrated with chemometrics analysis," *BioResources* 19(2), 3597-3613. DOI: 10.15376/biores.19.2.3597-3613

Walunj, A., Chen, Y., Tian, Y., and Zeng, Z. (2023). "Modeling soil–plant–machine dynamics using discrete element method: A review," *Agronomy* 13(5), article 1260. DOI: 10.3390/agronomy13051260

Wang, L., Zhang, S., Gao, Y., Cui, T., Ma, Z., and Wang, B. (2023). "Investigation of maize grains penetrating holes on a novel screen based on CFD-DEM simulation," *Powder Technology* 419, article 118332. DOI: 10.1016/j.powtec.2023.118332

Wang, X., Tian, H., Xiao, Z., Zhao, K., Li, D., and Wang, D. (2024). "Numerical simulation and experimental study of corn straw grinding process based on computational fluid dynamics–discrete element method," *Agriculture* 14(2), article 325. DOI: 10.3390/agriculture14020325

Xiao, Z., Tian, H., Zhang, T., Wang, D., Sheng, Y., Li, D., Liu, F., and Zhou, J. (2022). "Parameter calibration of discrete element numerical simulation for the dedusting sieve of corn straw feed," *Journal of China Agricultural University* 27(7), 172-183. DOI: 10.11841/j.issn.1007-4333.2022.07.16

Xue, X., Tian, H., Zhao, K., Yu, Y., Xiao, Z., Zhuo, C., and Sun, J. (2024). "Rapid lactic acid content detection in secondary fermentation of maize silage using colorimetric sensor array combined with hyperspectral imaging," *Agriculture* 14(9), article 1653. DOI: 10.3390/agriculture14091653

Yu, Y., Tian, H., Zhao, K., Guo, L., Zhang, J., Liu, Z., Xue, X., Tao, Y., and Tao, J. (2024). "Rapid pH value detection in secondary fermentation of maize silage using hyperspectral imaging," *Agronomy* 14(6), article 1204. DOI: 10.3390/agronomy14061204

Zhao, K., Tian, H., Ren, X., Yu, Y., Guo, L., Li, Y., Tao, Y., and Liu, F. (2024). "Screening of key volatile compounds characterizing the deterioration of maize silage during aerobic exposure," *Revista Brasileira de Zootecnia* 53, article e20230042. DOI: 10.37496/rbz5320230042

Zhou, P., Li, Y., Liang, R., Zhang, B., and Kan, Z. (2023). "Calibration of contact parameters for particulate materials in residual film mixture after sieving based on EDEM," *Agriculture* 13(5), article 959. DOI: 10.3390/agriculture13050959

Article submitted: October 17, 2024; Peer review completed: November 26, 2024; Revised version received and accepted: December 4, 2024; Published: December 11, 2024.
DOI: 10.15376/biores.20.1.1333-1344